

Metabolism of Pyridalyl in Rats After Repeated Oral Administration and a Simple PBPK Modeling in Brown and White Adipose Tissues

*Hirohisa Nagahori**, Haruyuki Matsunaga, Yoshitaka Tomigahara, Naohiko Isobe and Hideo Kaneko

Environmental Health Science Laboratory, Sumitomo Chemical Co., Ltd., 1-98, 3-Chome, Kasugade-Naka, Konohana-Ku, Osaka 554-8558, Japan

DMD #31914

Running Title: Metabolism of Pyridalyl in Rats and PBPK modeling

Corresponding author: Hirohisa Nagahori,

Environmental Health Science Laboratory, Sumitomo Chemical Co., Ltd., 1-98, 3-Chome, Kasugadenaka, Konohana-Ku, Osaka 554-8558, Japan

Tel.: 81-6-6466-5321. Fax: 81-6-6466-5442. E-mail: nagahori@sc.sumitomo-chem.co.jp.

Text pages: 14

Tables: 6

Figures: 5

References: 24

Abstract: 247 words

Introduction: 511 words

Discussion: 1524 words

Abbreviations used are: PBPK, physiologically based pharmacokinetics; f , unbound fraction; CL_{int} , hepatic intrinsic clearance; V , volume; C , concentration; P , permeability; Q , blood flow; K , equilibrium distribution ratio; F , absorption fraction, D , dose; k , absorption rate; DDT, dichlorodiphenyltrichloroethane; DDE, dichlorodiphenyldichloroethylene; PCB, Polychlorinated Biphenyl; TCDD, tetrachlorodibenzodioxin; SD, Sprague-Dawley; NMR, nuclear magnetic resonance; TLC, thin-layer chromatography; FAB, fast atom bombardment; MS, mass spectrometry; HPLC, high performance liquid chromatography; LSC, liquid scintillation counting; CYP, cytochrome P450; S-1812-DP, 3,5-dichloro-4-(3-(5-trifluoromethyl-2-pyridyloxy)propoxy)phenol, S-1812-AA, 2-[3,5-dichloro-4-[3-(5-trifluoromethyl-2-pyridyloxy)propoxy]phenoxy]acetic acid; S-1812-Py-OH, 2-(3-(2,6-dichloro-4-(3,3-dichloroprop-2-enyloxy)phenoxy)propoxy)-3-hydroxy-5-(trifluoromethyl)pyridine; HPHM, 3-[2,6-dichloro-4-(3,3-dichloroprop-2-enyloxy)phenoxy]propanol

DMD #31914

ABSTRACT

Male and female SD rats received repeated oral administration of ^{14}C -pyridalyl at 5 mg/kg/day daily for 14 consecutive days, and ^{14}C -excretion, ^{14}C -concentration in tissues and the metabolic fate were determined. Most ^{14}C was excreted into feces. The ^{14}C -concentrations in the blood and tissues attained steady state levels at days 6 - 10, while those in white adipose tissues increased until day 14. Tissue ^{14}C -concentrations were highest in brown and white adipose tissue (38.37 - 57.50 ppm) but 5.60 ppm or less in all the other tissues. Total ^{14}C -residues in blood and tissues on the 27th day after the first administration accounted for 2.6 - 3.2% of the total dose. A major fecal metabolite was resulting from *O*-dealkylation. Analysis of metabolites in tissues revealed that the majority of ^{14}C in perirenal adipose tissue and lungs was pyridalyl, accounting for greater than 90% and 60%, respectively, of the total, while a major metabolite in whole blood, kidneys, and liver was a dehalogenated metabolite. The experimental data were simulated with a simple physiologically based pharmacokinetics (PBPK) using four compartment models with assumption of lymphatic absorption and membrane permeability in adipose tissues. The different kinetics in brown and white adipose tissues were reasonably predicted in this model with large distribution volume in adipose tissues and high hepatic clearance in liver. Sex-related difference of pyridalyl concentration in liver was considered to be a result of different unbound fraction times the hepatic intrinsic clearance ($f \times \text{CL}_{\text{int}}$) of 1.8 and 12 L/h for male and female, respectively.

INTRODUCTION

Pyridalyl [2,6-dichloro-4-(3,3-dichloroallyloxy)phenyl 3-[5-(trifluoromethyl)-2-pyridyloxy]propyl ether] is a new class of insecticide for *Lepidoptera* and *Thysanoptera* (Sakamoto et al., 2004; Isayama et al., 2005). It has dichloropropenyl, dichlorophenyl and pyridyl groups in its structure and does not share structural similarity with other insecticides. The mode of action of pyridalyl have not been determined, it has toxicity to insect cells. Toxicity studies to mammal, including acute, chronic, oncogenicity, developmental, mutagenicity, and reproductive studies, have all been previously conducted with low acute toxicity, no oncogenicity and mutagenicity, and no teratogenicity observed (USEPA, 2008).

In previous studies, metabolism of [dichlorophenyl-¹⁴C]pyridalyl and [dichloropropenyl-¹⁴C]pyridalyl in rats was investigated in conjunction with toxicological safety evaluation (Nagahori et al., 2009ab). After administration of [dichlorophenyl-¹⁴C]pyridalyl or [dichloropropenyl-¹⁴C]pyridalyl to rats at 5 or 500 mg/kg, the radiocarbon was rapidly absorbed and relatively high levels were apparent in adipose tissue. Then, ¹⁴C was rapidly excreted mainly into feces (>99% of the dose) for [dichlorophenyl-¹⁴C]pyridalyl and feces (~ 70%) , urine (~10%) and expired air (~10%) for [dichloropropenyl-¹⁴C]pyridalyl. Ether cleavage was the major biotransformation reaction.

¹⁴C-concentrations decreased relatively slowly in adipose tissue and skin, and ¹⁴C in adipose tissue was primarily accounted for by pyridalyl itself. To clarify the accumulation and decrease of pyridalyl in rat body, time course of ¹⁴C-concentration in tissues including brown and white fat during and after repeated oral administration of pyridalyl is measured. The high concentration in adipose tissue might have been caused by the lipophilic nature of pyridalyl (log P = 8.1). Lipophilic compounds such as dieldrin, DDT (DDE), PCB and TCDD are also known to become distributed to adipose tissue and eliminated slowly. However, pyridalyl has a different nature. Residual ¹⁴C in adipose tissue 7 days after administration of pyridalyl was 2% of the dose, in contrast to values for lipophilic compounds such as dieldrin, DDT (DDE), PCB and TCDD of >6%, 53.03%, 50 to 70% and 10 to 20%, respectively (Hayes, 1974; Mühlebach et al., 1991; Matthews and Tuey, 1980; Abraham et al., 1988). Pyridalyl has an ether bond which is easily cleaved, while dieldrin, DDT (DDE) and PCB are more resistant to degradation. In the current study, we determined the rate and extent of ¹⁴C accumulation in adipose tissue (brown and white fat) after repeated oral administration of pyridalyl and the results were compared with other lipophilic compounds to clarify differences in accumulation properties.

Pyridalyl was rapidly metabolized to form S-1812-DP in liver after administration, and then excreted rapidly (Nagahori et al., 2009a). To clarify the distribution profile and metabolic stability, physiologically based pharmacokinetic (PBPK) models are useful analytical tools. Therefore, also utilized such a model for fitting the observed data and model parameters were determined to

DMD #31914

quantitatively assess the pharmacokinetics of pyridalyl in rats. Relevant data for lipophilic compounds, such as TCDD, chlordecone, p,p'-DDE and hexachlorobenzene have been generated previously (Roth et al., 1993; Emond et al., 2004; Wang et al., 2000; Evans et al., 2000; Li et al., 1995; Belfiore et al., 2007; You and Gazi, 1999; Lu et al., 2006), allowing direct comparison. The present report thus deals with metabolism (^{14}C -excretion into feces, urine, expired air, ^{14}C -concentrations in tissues including brown and white fat, and amounts of metabolites in excreta and tissue) of [dichlorophenyl- ^{14}C]pyridalyl in male and female rats during and after repeated oral administration for 14 consecutive days at 5 mg/kg/day to determine the extent of accumulation and elimination of accumulated radioactivity. In addition, pyridalyl concentrations in tissues were analyzed by a simple PBPK modeling to clarify the distribution property and metabolic stability of pyridalyl and to facilitate comparison with other lipophilic compounds.

MATERIALS AND METHODS

Chemicals. [dichlorophenyl-¹⁴C]pyridalyl was prepared at the Environmental Health Science Laboratory (EHLS) of Sumitomo Chemical, Co., Ltd (Takarazuka). with a specific activity of 10.2 MBq/mg. Labeled compound was purified with thin layer chromatography (TLC) before use and the radiochemical purity was >98.8%. Unlabeled pyridalyl (purity: 99.7%) was also obtained from our company and analyzed by NMR spectrometry; ¹H-NMR (CD₃OD, 270 MHz, ppm) δ6.29 (1H, t, *J* = 6.2 Hz), 4.66 (2H,m), 6.97 (2H,m), 4.15 (2H, t, *J* = 5.6 Hz), 2.30 (2H, m), 4.66 (2H, m), 6.97 (1H, m), 7.94 (1H, dd, *J* = 8.5, 2.3 Hz), 8.49 (1H, d, *J* = 2.3 Hz); ¹³C-NMR (CD₃OD, 67.5 MHz) δ126, 64, 117, 131, 71, 31, 67, 112, 137, 146 ppm. FAB-MS showed a molecular ion peak at *m/z* 490[M+H]⁺. Authentic standards (S-1812-DP, S-1812-Py-OH, HPHM and S-1812-AA) were prepared at EHLS. Other chemicals were all reagent grade.

Thin layer chromatography (TLC) analysis. Identification and quantification of metabolites were conducted using a solvent system of hexane/toluene/acetic acid (3:15:2, v/v/v, developed twice). Unlabeled pyridalyl and authentic standards on TLC plates was detected by viewing under UV light (254 nm) and radioactive metabolites by autoradiography using imaging plates processed with a BAS2000 Bio-image Analyzer (Fuji Photo Film, Kanagawa, Japan). Pyridalyl and S-1812-DP was isolated using the same solvent system for further identification by HPLC.

HPLC analysis. Purification of isolated pyridalyl and S-1812-DP was conducted using an L-6200 type intelligent pump (Hitachi, Tokyo, Japan), an L-4000 UV detector (Hitachi), an LB 507A HPLC Radioactivity Monitor (Berthold, Germany), and an 805 data station (Japan Millipore Limited, Tokyo). The metabolites were purified using an ODS column (cosmosil, 4.6 mm I.D. x 15 cm, Nacalai Tesque, Japan) and a guard column (Waters Guard-Pak, μBondapak C₁₈, Millipore Corporation, USA) with mobile phases of acetonitrile/1% acetic acid in water (gradients, 0:100 (0 - 5 min), 20:80 (10 - 30 min) 100:0 (35 min)). The flow rate was 1.0 mL/min. Purified pyridalyl and S-1812-DP were identified by HPLC cochromatography with authentic standards using the same conditions as described above. The wavelength of the UV detector was set at 254 nm.

Radioanalysis. Radioactivity in organosoluble fractions or urine was quantified by liquid scintillation counting (LSC) giving disintegrations per minute (dpm) by the external standard method with a Tri-Carb 2500TR Liquid Scintillation Analyzer (PerkinElmer, MA). Samples (100 - 300 mg) of fecal homogenates, unextractable fecal residues and tissues were combusted with a sample oxidizer (Tri-Carb

DMD #31914

307, PerkinElmer) prior to LSC after air-drying (combustion-LSC method). Quantification of radiocarbon on TLC plates was conducted with scraping methods.

Animal treatment. Seven groups of three male and three female Crj:CD(SD) rats at the age of 6 weeks were purchased from Charles River Japan Inc. (Kanagawa, Japan). All animal experiments were conducted in accordance with the Guidelines for Proper Conduct of Animal Experiments (Science Council of Japan). Animals that showed normal weight gain and no abnormal clinical symptoms during 7 days of quarantine and acclimation were selected for dosing. The in-life portion of the study was conducted under the following environmental conditions: room temperature, 20 - 26 °C; relative humidity, 55 ± 10%; ventilation, 10 air exchanges per hour; and artificial lighting from 8:00 am to 8:00 pm. Animals had free access to pelleted diet and water through the study. Seven groups (designated as groups A to G) of three male and three female rats were orally dosed [dichlorophenyl-¹⁴C]pyridalyl (2.02 x 10⁷ dpm/mg) in corn oil at 5 mL/kg with 5 mg/kg/day for 1, 6, 10 days for groups A to C, respectively, and 14 days for groups D to G and housed in aluminum cages or glass metabolism cages (only for group G).

Metabolism study. The animals of the group G were used for metabolism studies. Feces and urine were separately collected daily to day 17 and once every two days thereafter (days 19 to 27). Following the collection of feces and urine, the cage was washed with water to recover ¹⁴C (cage-wash samples).

The urine and cage-wash samples were weighed and then duplicate aliquots of each sample were radioassayed by LSC. Radioactivity in the cage-wash samples was included in the urinary excretion. The fecal samples of individual rats were separately homogenized with an approximately 3-fold volume of water, and then duplicate aliquots were combusted for radioanalysis.

Tissue distribution study. Rats were euthanized with collection of blood from the abdominal artery at 1 day after the last administration for groups A to C, and after 1, 4, 7 and 14 days, respectively, for groups D to G. Their organs and tissues were dissected out and plasma and blood cells were separated by centrifugation (2000g, 10 min). Blood was collected in plastic vials containing aliquots of heparin (Nacalai Tesque, Inc.). An aliquot of collecting blood (ca. 1 - 3 g) was centrifuged at 2000 g for 10 min at 4 °C in order to separate the plasma from red blood cells. Duplicate aliquots of whole blood, plasma, red blood cells, and each tissue were measured by a combustion-LSC method. However, the average ¹⁴C-concentration in lungs of two female rats was used for day 6. The ¹⁴C-concentration in lungs of the third female rat on day 6 was not included because of a value about 10 times higher than those in all other lungs of males and females.

Chromatographic analysis of metabolites. Equal percentages of 0 - 3 day fecal homogenates were pooled by sex, and were mixed with an approximately 5-fold volume of acetone. The homogenates were centrifuged at 2000 g for 10 minutes at 4 °C. The supernatants were collected by decantation and the precipitates were extracted twice with acetone. The residues from the acetone extraction were then extracted three times with a 5-fold volume of a mixture of methanol/water (9:1, v/v) in the manner described above. Each extract was combined, weighed and then duplicate aliquots were radioassayed by LSC. Each residue was mixed with a 3-fold volume of water, weighed and then duplicate aliquots were combusted to determine the extraction efficiency for ¹⁴C in feces. The fecal homogenates for days 11 - 14 were processed similarly. The fecal and tissue extracts were concentrated and analyzed by TLC.

Equal percentages of 0 - 3 day urine were pooled by sex and analyzed by TLC. Urine from days 11 - 14 was processed similarly.

Blood (ca. 1g) of each rat in the group D was pooled for each sex. Samples (ca. 0.3 -0.5 g) of perirenal adipose tissue, kidneys, liver and lungs of each rat in the group D were also similarly pooled for each sex. Pooled tissues were extracted with the same procedure as for fecal extraction described above.

The metabolites on TLC plates were quantified by the scraping-LSC method. Radioactivity in areas where no discrete spot or band was detected on the TLC autoradiograms was included in “others”. Urinary, fecal and tissue metabolites were identified by TLC co-chromatography with authentic standards. Additionally, major fecal metabolites (pyridalyl and S-1812-DP) were isolated by TLC and identified by HPLC co-chromatography with corresponding authentic standards.

PBPK model development. The model was based on data from two studies, an earlier single oral administration (Nagahori et al., 2009a) and the present repeated oral administration of pyridalyl. The model structure included the blood, liver, white adipose tissue, brown adipose tissue and the rest of body with assumption of lymphatic absorption and membrane permeability in adipose tissues (Figure 1). The general mass balance equation of the white (w) and brown adipose tissue (b) should be expressed as Equation A: The mass balance for the concentrations, C_x, is

$$V_x \times \frac{dC_x}{dt} = \frac{P_x}{1 + \frac{P_x}{Q_x}} (C_a - \frac{C_x}{K_x}) \quad (A)$$

where x stands for w, b and r, t is time, V_x is the volume of each compartment, Q_x is the blood flow rate to each compartment, K_x is the equilibrium distribution ratio, C_a is the concentration in blood, P_x is the permeability and C_x is the concentration in each compartment.

In and rest of the body (r), the mass balance for the concentrations, C_r, is

$$V_r \times \frac{dC_r}{dt} = Q_r \times \left(C_a - \frac{C_r}{K_r} \right) \quad (\text{B})$$

In the liver (l), the mass balance for the concentration, Cl, is

$$V_l \times \frac{dCl}{dt} = Q_l \times \left(C_a - \frac{Cl}{K_l} \right) - f \times CL_{int} \times \frac{Cl}{K_l} \quad (\text{C})$$

where f is unbound fraction and CL_{int} is the hepatic intrinsic clearance.

In the blood (a), the mass balance for the concentration, Ca, is

$$V_a \times \frac{dC_a}{dt} = \frac{P_w \times C_w}{\left(1 + \frac{P_w}{Q_w}\right) \times K_w} + \frac{P_b \times C_b}{\left(1 + \frac{P_b}{Q_b}\right) \times K_b} + \frac{Q_l \times Cl}{K_l} + \frac{Q_r \times C_r}{K_r} - C_a \times \left(\frac{P_w}{1 + \frac{P_w}{Q_w}} + \frac{P_b}{1 + \frac{P_b}{Q_b}} + Q_l + Q_r \right) + F \times D \times k \times e^{-k \times t} \quad (\text{D})$$

where F is the absorption fraction, D is the oral dose, k is the absorption rate. Pyridalyl concentrations in each compartment after single oral administration were calculated by the Runge-Kutta-Gill method (Hanano, 1987). Pyridalyl concentrations in each compartment after repeated oral administration were calculated by a superposition technique with concentrations after the single oral administration.

Model parameters are shown in Table 1. The absorption fraction, F, was experimentally set at 0.4 at first administration, and 0.8 thereafter (see Discussion section; absorption fraction becomes higher after repeated dose). Absorption fraction was calculated as follows using the amount of metabolites in excreta. About 40% of ¹⁴C in excreta were metabolites and about 60% of ¹⁴C were unchanged pyridalyl (Nagahori et al., 2009a). Since unchanged pyridalyl in feces was considered to be unabsorbed pyridalyl and metabolites in excreta were formed in the body after absorption, absorption fraction after single oral administration was set at 0.4. Absorption fraction after repeated oral absorption was calculated with the same calculation using data in the Table 5. The values of equilibrium coefficient (K), absorption rate (k), permeability (P) and unbound fraction times the hepatic intrinsic clearance (f x CL_{int}) were optimized by model fitting to the data sets as follows. The values of equilibrium coefficient (K) and absorption rate (k) were initially obtained from Table 6 and data of TCDD (Emond et al., 2004), respectively, and permeability (P) was presumed from distribution and elimination rate of ¹⁴C-concentration in adipose tissues (Tables 2 and 3 of the present study). ¹⁴C-concentration in adipose tissues was considered as the pyridalyl concentration, since the majority of ¹⁴C in adipose tissue was due to pyridalyl itself. First, the combined parameter, unbound fraction times the hepatic intrinsic clearance (f x CL_{int}), were optimized by model fitting to the data sets of ¹⁴C-concentration in adipose tissues and pyridalyl concentrations in liver and blood at 14th day (Table 6), since unbound fraction and hepatic intrinsic clearance were not accurately determined due to low ¹⁴C-concentration of pyridalyl in blood. Then, K, k, P and f x CL_{int} were refined and optimized sequentially for several times using ¹⁴C-concentration and pyridalyl concentrations in adipose tissues, liver and blood after repeated oral administration and corrected pyridalyl concentration calculated from ¹⁴C-concentration in

DMD #31914

the earlier study (Nagahori et al., 2009a). Correction factors were used for calculation of corrected pyridalyl concentration in adipose tissues, liver and blood using the equation, corrected pyridalyl concentration = correction factor x total ^{14}C concentration in tissues. Correction factors of adipose tissues, liver and blood were 1, 0.3, and 0.3, respectively, for males and 1, 0.06 and 0.3, respectively, for females, derived from data in Table 6. The optimized K and P are shown in Table 1. The optimized absorption rate (k) was 0.05 h^{-1} . Optimized unbound fraction times the hepatic intrinsic clearance (f x CLint) were 1.8 L/h and 12 L/h, respectively, for males for females.

RESULTS

1. ^{14}C -Excretion

Feces and urine were collected and radioassayed daily or once every two days during and after repeated oral administration of [dichlorophenyl- ^{14}C]pyridalyl at 5 mg/kg/day to male and female rats daily for 14 consecutive days. Profiles of ^{14}C -administration and ^{14}C -excretion into feces and urine were calculated as percentages of the total dose, and are shown in Figure 2. Most ^{14}C was excreted into feces, accounting for 91.5 - 94.5% of the total dose within 27 days, and that into urine 2.0 - 4.4% of the total dose. Total ^{14}C -excretion within 27 days after first administration was approximately 96 - 97% of the total dose. ^{14}C -Excretion showed no remarkable sex-related difference.

2. ^{14}C -distribution to blood and tissues

Blood and tissues were collected and radioassayed at days 1, 6, 10, 14, 17, 20, and 27. ^{14}C -Concentrations in blood and tissues are shown in Tables 2 and 3 for males and females, respectively, and biological half-life times of ^{14}C in tissues of male and female rats are shown in Table 4. The ^{14}C -concentrations in blood and tissues, except for white adipose tissue (perirenal and testicular sites), generally increased in proportion with the number of administrations at days 1 - 6 or 1 - 10, and then reached a plateau. The ^{14}C -concentrations in white adipose tissues increased until day 14. Adipose tissues (brown and white) showed the highest concentrations of 38.37 - 57.50 ppm, whereas ^{14}C -concentrations in other tissues were relatively low (5.60 ppm or less). The ^{14}C -concentrations in the tissues except for white adipose tissues generally showed biphasic decrease with biological half-lives of 1 - 5 days (α phase) and of 4 - 24 days (β phase), while elimination from white adipose tissue was exponential with biological half-lives of 10 - 15 days. Total ^{14}C -residues at day 27 after first administration were calculated as the sums of the radioactivity found in blood and tissues, accounting for 2.6 - 3.2% of the total dose. Total ^{14}C -recovery in excreta, blood and tissues was approximately 99% of the total dose. The ^{14}C -concentrations in blood and tissues showed no remarkable sex-related difference.

5. Metabolites in feces and urine

The urine samples and fecal extracts were analyzed by TLC. Table 5 shows data for metabolite distribution as percentages of the total dose between days 0 - 3 and days 11 - 14. S-1812-DP was detected as the major metabolite, accounting for about 6 - 10% of the total dose. Other metabolites each accounted for less than 1% of the total dose. Pyridalyl excretion between days 0 - 3 was higher than that between days 11 - 14, accounting for about 7 - 8% and 5 - 6% of the total dose, respectively. The lower pyridalyl excretion at days 11-14 might indicate enhanced absorption with repeated oral doses.

Absorption fractions (100 –percentage of pyridalyl in excreta) were calculated to be approximately 60% for 0 - 3 day and 80% for 11 - 14 day. On the other hand, metabolite distribution shown as % of metabolites did not remarkably change between days 0 - 3 and days 11 - 14. No sex-related difference in the metabolite distribution was observed in males and females.

5. Metabolites in tissues

Blood and tissue extracts were analyzed by TLC. Table 6 shows the metabolite distribution as μg equivalents of pyridalyl in g tissue (ppm). The majority of ^{14}C in perirenal adipose tissue and lungs was pyridalyl, accounting for greater than 90% and 60% of the total radioactive residues, respectively, whereas S-1812-AA was the major metabolite in whole blood, kidneys, and liver. Though the pyridalyl concentration in liver was much lower in females, no other remarkable sex-related difference in the metabolite distribution was observed.

6. Simulation

Pyridalyl concentrations in adipose tissues, liver and blood were reasonably predicted using a simple PBPK model shown in Figure 1 and parameters shown in Table 1 and Materials and Methods section. Figure 3 presents the model predictions of pyridalyl concentration in adipose tissue, liver and blood and the corrected experimental data for ^{14}C concentrations in adipose tissue, liver and blood of male and female rats after single oral administration of [dichlorophenyl- ^{14}C]pyridalyl at 5 mg/kg. Figure 4 presents the model predictions of pyridalyl concentration in adipose tissues, liver and blood and the corrected experimental data for ^{14}C concentrations in adipose tissues and the pyridalyl concentrations in blood and liver of male and female rats during and after repeated oral administration of [dichlorophenyl- ^{14}C]pyridalyl at 5 mg/kg/day for 14 consecutive days. A large distribution volume in adipose tissues and high hepatic clearance in liver were important for precise prediction of pyridalyl concentration in each tissue. The prediction of the pyridalyl concentrations in adipose tissues reasonably agreed with the experimental data of ^{14}C in adipose tissues, considering majority of ^{14}C in adipose tissues are pyridalyl. The different kinetics in brown and white adipose tissues were reasonably predicted in this model. The prediction of the pyridalyl concentrations in blood and liver were consistent with the experimental data. The remarkable sex-related difference in liver and slight difference in adipose tissues was reasonably predicted using unbound fraction times hepatic intrinsic clearance ($f \times \text{CL}_{\text{int}}$) of 1.8 and 12 L/h in males and females, respectively.

DISCUSSION

In the present study of metabolic fate and tissue accumulation of [dichlorophenyl-¹⁴C]pyridalyl during and after repeated oral administration of [dichlorophenyl-¹⁴C]pyridalyl at 5 mg/kg/day to male and female rats daily for 14 consecutive days, the radiocarbon was rapidly absorbed and ¹⁴C-concentrations showed differing profiles among white adipose, brown adipose, and other tissues. In all but the white adipose case a steady-state was reached around days 6 - 10. In white adipose tissue increase continued until day 14. The ¹⁴C-concentration in the white adipose tissues was relatively high (approximately 38 - 43 ppm) and similar to that in brown adipose tissue (approximately 39 - 58 ppm). However, ¹⁴C-concentrations in other tissues were relatively low (<5.60 ppm). ¹⁴C-Concentration in white adipose tissues decreased slowly after termination of dosing, while those in other tissues decreased biphasically and rapidly. ¹⁴C was rapidly excreted into mainly feces, comparable with the earlier single oral dose study (Nagahori et al., 2009a). Cumulative ¹⁴C-distribution at day 27 was 92 - 95%, 2 - 4% and 3% of the total dose for feces, urine and tissues, respectively, with total ¹⁴C recoveries of 99%. S-1812-DP was detected as the major metabolite in excreta, again in line with the single oral dose study (Nagahori et al., 2009a). Small amounts of S-1812-Py-OH, HPHM, S-1812-AA, and other metabolites were detected in excreta. The majority of ¹⁴C in perirenal adipose tissue and lungs was pyridalyl, whereas that in whole blood, kidneys, and liver was S-1812-AA. No marked sex-related differences were observed in ¹⁴C-elimination, the ¹⁴C-distribution and the metabolite profile, except for liver pyridalyl concentration.

¹⁴C-elimination (>90% of fecal excretion), the ¹⁴C-distribution (relatively high concentration in fat) and metabolite profile in excreta (mainly S-1812-DP) appear to be similar with single low, single high (Nagahori et al., 2009a) and repeated oral administration schedules. In addition, pharmacokinetics were proportional to dose in both high (500 mg/kg) and low dose (5 mg/kg) previous single oral dose studies (Nagahori et al., 2009a). The results thus indicate that metabolism, distribution and excretion of pyridalyl were not affected by increase of dose to 500 mg/kg or repeated doses. Only one difference was that fecal pyridalyl content was decreased with repeated oral administration. The results indicate that the absorption fraction increased with repeated oral administration. The absorption fraction with single oral dose was approximately 40% in the previous single oral dose study calculated from excreted fecal metabolites (Nagahori et al., 2009a). With our repeated oral doses, the absorption fraction was estimated to be approximately 60% and 80% at 0 - 3 and 11 - 14 days, respectively, since the percentage of fecal pyridalyl considered unabsorbed was approximately 40% and 20% in 0 - 3 and 11 - 14 day feces. The observed increase in the absorption fraction might have been caused by repeated administration of the vehicle, corn oil, which produces high concentrations of chylomicrons in the

lymph (Cheema et al., 1987). Increase of the absorption fraction after oil administration was also observed with other lipophilic chemicals, such as DDT (Palin et al., 1982) which are absorbed *via* the lymphatic system. Though the absorption route of pyridalyl was here not identified, its lipophilicity and increase of absorption fraction suggest lymphatic absorption of pyridalyl. This would reasonably explain the rapid distribution of pyridalyl to tissues (fat) and blood without high levels in the liver.

¹⁴C-distribution and elimination in white adipose tissue and brown adipose tissue were significantly different, though the highest ¹⁴C-concentrations in these tissues were similar. In our current results, brown adipose tissue showed the more rapid distribution and elimination. The difference appeared to be related to blood flow and distribution volume. Data for the tissue volume, partition coefficient and blood flow of these tissues are shown in Table 1. The tissue volume of brown fat was smaller than that of white fat. The partition coefficient of pyridalyl in brown fat ($P_b = 1000$) was fitted to be only slightly lower than that of white fat ($P_w = 1200$). The partition of lipophilic compound in these tissues is reported to be controlled by lipid contents and a lower partition coefficient in brown adipose tissue was also observed with TCDD (Roth et al., 1994). Smaller distribution volume of brown fat is based on the smaller volume and lower partition coefficient of brown adipose tissue. Higher blood flow and smaller distribution volume could cause rapid distribution and elimination in brown fat. The same distribution profile was observed with lipophilic compounds, such as TCDD (Weber et al., 1993), but this is the first report for prediction of pharmacokinetics of more lipophilic and higher clearance compound using a simple PBPK model including brown and white adipose tissues.

The fact that ¹⁴C-concentrations decreased relatively slowly in adipose tissue might have been caused by the lipophilic nature of pyridalyl ($\log P = 8.1$). High lipophilicity of pyridalyl combined with a low blood flow rate in adipose tissue (0.1 L/h) might result in a high distribution volume. The current PBPK model of pyridalyl could simulate these pharmacokinetics, in agreement with experimental data for ¹⁴C in white adipose tissues using a high partition coefficient ($K_w = 1200$) and high permeability ($P_w/Q_w = 1.3$). Partition coefficient and permeability of pyridalyl is higher than that of other highly lipophilic compounds, such as TCDD, and the lipophilic nature might result in a prolonged time to steady state and a delayed biological half-life. High partition rate is consistent with the difference of pyridalyl concentration (about 1200 times) in adipose tissue and in blood at steady state (from Table 6), and high permeability is consistent with fast distribution of pyridalyl to adipose tissue within 1 day (Nagahori et al., 2009a). The elimination rate from white fat calculated with the equation, ($P_w / (K_w \times V_w \times (1 + P_w / Q_w))$) (from equation A), was very low, 0.0028 h^{-1} and was comparable to that published for TCDD (0.0016 h^{-1}) (Emond et al., 2004).

DMD #31914

Though elimination from adipose tissue was slow, ^{14}C residues in tissue were low at about 3%. This contrasts with values of >6%, 53.03%, 50 to 70% and 10 to 20%, respectively, for lipophilic compounds such as dieldrin, DDT (DDE), PCB and TCDD (Hayes, 1974; Mühlebach et al., 1991; Matthews and Tuey, 1980; Abraham et al., 1988). Though elimination of these lipophilic compounds from adipose tissue was similar, relatively high residue of these compounds in adipose tissue might be due to metabolic stability. Pyridalyl has an ether bond which is readily cleaved, while dieldrin, DDT (DDE) and PCB are more resistant to degradation. Pyridalyl is rapidly metabolized to form S-1812-DP in liver after administration, and then seems to be excreted rapidly. In the current PBPK model, unbound fraction times the hepatic intrinsic clearance of pyridalyl was estimated to be 1.8 to 12 L/h, much higher than with other lipophilic compounds, such as, chlordecone (0.005 L/hr; Belfiore et al., 2007), DDT (DDE, 0 L/h; You et al., 1999) and hexachlorobenzene (0.00195 L/hr; Lu et al., 2006). Hepatic clearance of pyridalyl was predominantly determined by hepatic blood flow (flow limited) and calculated to be 0.6 to 0.9 L/h with the equation $(Ql \times f \times CL_{int} / (Ql + f \times CL_{int}))$. This high hepatic intrinsic clearance of pyridalyl could have been responsible for the lower accumulation of pyridalyl in adipose tissues.

The simulated low pyridyl concentration in blood (<0.1 ppm) is consistent with high hepatic clearance. Though the free fraction of pyridalyl in blood was not confirmed, it might be expected to be low, due to the high partition coefficients in adipose tissue and liver. Low concentration of free pyridalyl resulted in low distribution of pyridalyl to tissues except fat and liver. One reason for low toxicity could be the high lipophilic nature of pyridalyl. When added to the fact that pyridalyl was rapidly metabolized and eliminated from the body, this provides an explanation for the low toxicity of pyridalyl was in contrast to high toxicity of TCDD.

Though a marked sex related difference was not observed in ^{14}C -elimination and the ^{14}C -distribution, pyridalyl concentrations in liver did markedly differ between males and females. In addition, slight sex-variation was observed in ^{14}C concentrations in adipose tissue. These differences could be simulated with increase of unbound fraction times hepatic intrinsic clearance ($f \times CL_{int}$) in female rats from 1.8 to 12 L/h. Though the clearance was approximately 7 times higher than in males, the slight difference in ^{14}C -concentrations in adipose tissue might be due to blood flow limited hepatic clearance of pyridalyl. Difference in hepatic intrinsic clearances affected only hepatic pyridalyl concentrations. These differences presumably were related to reported variation in activity and expression of cytochrome P450, such as CYP2C12, CYP2C7 and CYP2A1, between the sexes (Pampori and Shapiro, 1999). These enzymes could be involved in metabolism of pyridalyl. However, we have not yet

DMD #31914

conducted an in vitro metabolism study for identification of metabolizing enzyme, so this remains to be tested.

Absorbed ^{14}C was rapidly eliminated into feces as S-1812-DP, an ether cleaved metabolite of pyridalyl. The metabolic profile was almost same as that in the single oral study. The hydroxyl group in S-1812-DP can be conjugated to form a glucuronide or sulfate in liver after absorption and conjugated S-1812-DP is readily excreted into feces via the bile. S-1812-DP was detected as a major metabolite in excreta, and was also the major form in the single oral dose study (Nagahori et al., 2009a). Small amounts of S-1812-Py-OH, HPHM, S-1812-AA, and other metabolites were detected in excreta. The majority of ^{14}C in perirenal adipose tissue and lungs was pyridalyl, whereas that in whole blood, kidneys, and liver was S-1812-AA. Proposed metabolic pathways are shown in Figure 5.

REFERENCES

Abraham K, Krowke R, and Neubert D (1988) Pharmacokinetics and biological activity of 2,3,7,8-tetrachlorodibenzo-p-dioxin. 1. Dose-dependent tissue distribution and induction of hepatic ethoxyresorufin O-deethylase in rats following a single injection. *Arch Toxicol* **62**: 359-68.

Belfiore CJ, Yang RSH, Chubb LS, Lohitnavy M, Lohitnavy OS, Andersen ME (2007) Hepatic sequestration of chlordecone and hexafluoroacetone evaluated by pharmacokinetic modeling. *Toxicology* **234**: 59–72.

Cheema M, Palin KJ, Davis SS (1987) Lipid vehicles for intestinal lymphatic drug absorption. *J Pharm Pharmacol* **39**: 55-6.

Emond C, Birnbaum LS, DeVito MJ (2004) Physiologically based pharmacokinetic model for developmental exposures to TCDD in the rat. *Toxicol Sci* **80**: 115-33.

Evans MV, Andersen ME (2000) Sensitivity Analysis of a Physiological Model for 2,3,7,8-Tetrachlorodibenzo-p-dioxin (TCDD): Assessing the Impact of Specific Model Parameters on Sequestration in Liver and Fat in the Rat. *Toxicol Sci* **54**: 71–80.

Hanano M (1987) *Pharmacokinetics*, p47, Nanzando, Tokyo.

Hayes WJ Jr (1974) Distribution of dieldrin following a single oral dose. *Toxicol Appl Pharmacol* **28**: 485–492.

Isayama S, Saito S, Kuroda K, Umeda K, Kasamatsu K. (2005) Pyridalyl, a novel insecticide: potency and insecticidal selectivity. *Arch Insect Biochem Physiol* **58**:226-233.

Li X, Weber LW, Rozman KK (1995) Toxicokinetics of 2,3,7,8-tetrachlorodibenzo-p-dioxin in female Sprague-Dawley rats including placental and lactational transfer to fetuses and neonates. *Fundam Appl Toxicol* **27**:70-6.

Lu Y, Lohitnavy M, Reddy MB, Lohitnavy O, Ashley A, Yang RSH (2006) An Updated Physiologically Based Pharmacokinetic Model for Hexachlorobenzene: Incorporation of Pathophysiological States following Partial Hepatectomy and Hexachlorobenzene Treatment. *Toxicol Sci* **91**: 29–41.

Matthews HB and Tuey DB (1980) The effect of chlorine position on the distribution and excretion of four hexachlorobiphenyl isomers. *Toxicol Appl Pharmacol* **53**: 377-88.

Mühlebach S, Moor MJ, Wyss PA, and Bickel MH (1991) Kinetics of distribution and elimination of DDE in rats. *Xenobiotica* **21**: 111-20.

Nagahori H, Saito K, Tomigahara Y, Isobe N, Kaneko H (2009a) Metabolism of Pyridalyl in Rats. *Drug Metab Dispos* **37**:2284-9.

Nagahori H, Tomigahara Y, Isobe N, Kaneko H (2009b) Metabolism of Pyridalyl in Rats: Excretion, Distribution and Biotransformation of Dichloropropenyl-Labeled Pyridalyl. *J Agric Food Chem* **57**:10845-51.

Palin KJ, Wilson CG, Davis SS, Phillips AJ (1982) The effect of oils on the lymphatic absorption of DDT. *J Pharm Pharmacol* **34**:707-10.

Pampori NA, Shapiro BH (1999) Gender Differences in the Responsiveness of the Sex-Dependent Isoforms of Hepatic P450 to the Feminine Plasma Growth Hormone Profile. *Endocrinology* **140**: 1245-54.

Roth WL, Weber LW, Stahl BU, Rozman K (1993) A pharmacodynamic model of triglyceride transport and deposition during feed deprivation or following treatment with 2,3,7,8-tetrachlorodibenzo-p-dioxin (TCDD) in the rat. *Toxicol Appl Pharmacol* **120**: 126-37.

Roth WL, Ernst S, Weber LW, Kerecsen L, Rozman KK (1994) A pharmacodynamically responsive model of 2,3,7,8-tetrachlorodibenzo-p-dioxin (TCDD) transfer between liver and fat at low and high doses. *Toxicol Appl Pharmacol* **127**: 151-62.

Sakamoto N, Saito S, Hirose T, Suzuki M, Matsuo S, Izumi K, Nagatomi T, Ikegami H, Umeda K, Tsushima K, and Matsuo N (2004) The discovery of pyridalyl: a novel insecticidal agent for controlling lepidopterous pests. *Pest Management Science* **60**: 25-34.

US Environmental Protection Agency (USEPA) (2008) Pesticide Fact Sheet: Pyridalyl.

Wang X, Santostefano MJ, DeVito MJ, Birnbaum LS (2000) Extrapolation of a PBPK model for dioxins across dosage regimen, gender, strain, and species. *Toxicol Sci* **56**: 49-60.

Weber LW, Ernst SW, Stahl BU, Rozman K (1993) Tissue distribution and toxicokinetics of 2,3,7,8-tetrachlorodibenzo-p-dioxin in rats after intravenous injection. *Fundam Appl Toxicol* **21**: 523-34.

DMD #31914

You L, Gazi E, Archibeque-Engle S, Casanova M, Conolly RB, Heck H (1999) Transplacental and Lactational Transfer of p,p'-DDE in Sprague–Dawley Rats. *Toxicol Appl Pharmacol* **157**: 134–44.

FIGURE CAPTIONS

Figure 1. Diagram of the PBPK model after single oral administration of [dichlorophenyl-¹⁴C]pyridalyl to rats.

Figure 2. Cumulative ¹⁴C-excretion into urine, feces during and after repeated oral administration of [dichlorophenyl-¹⁴C]pyridalyl to male (A) and female (B) rats at 5 mg/kg/day for 14 successive days. ↑; administration of [dichlorophenyl-¹⁴C]pyridalyl at 5mg/kg.

Figure 3. Simulated and experimental pyridalyl concentration in perirenal adipose tissue, liver and blood after single oral administration of [dichlorophenyl-¹⁴C]pyridalyl to male (A) and female (B) rats at 5 mg/kg. -:simulated data. Corrected pyridalyl concentrations were derived from ¹⁴C-concentrations data in the previous study (Nagahori et al., 2009a) using the following correction factor. Correction factors of adipose tissues, liver and blood were 1, 0.3, and 0.3, respectively, for males and 1, 0.06 and 0.3, respectively, for females (See Table 6).

Figure 4. Simulated and experimental pyridalyl concentration in adipose tissue (perirenal, testicular and brown), liver and blood after repeated oral administration of [dichlorophenyl-¹⁴C]pyridalyl to male (A) and female (B) rats at 5 mg/kg/day daily for 14 successive days. Experimental pyridalyl concentrations in adipose tissues were derived from ¹⁴C-concentrations data in Tables 2 and 3. Experimental pyridalyl concentrations in blood and liver were derived from Table 6. -:simulated data.

Figure 5. Proposed metabolic pathways for [dichlorophenyl-¹⁴C]pyridalyl to rats.

TABLES

Table 1 Parameter values for the PBPK model

	% body weight (250g rat) ^{a)}	Compartment volume (V, mL)	% of cardiac output (311.4 mL/min/kg) ^{b)}	Blood flow (Q, L/h)	Partition coefficient (K) ^{c)}	Permeability L/h) ^{d)}
Blood	5.4	13.5	-	-	-	-
Liver	4.86	12.2	21.0	0.981	150	-
White adipose tissue	6.25	15.6	2.00	0.0934	1200	$P_w / Q_w = 1.3$
Brown adipose tissue	1.25	3.13	3.00	0.140	1000	$P_b / Q_b = 0.4$
Rest of body	73.2	183	74.0	3.46	1	-

- a) Values from the previous literature (Roth et al., 1993) and the volume fraction for the rest of the body was estimated from the total volume fraction of 91% (Emond et al., 2004).
- b) Values are from the previous literature (Roth et al., 1993) including the % of cardiac output of the rest of the body (Emond et al., 2004).
- c) Values were initially obtained from Table 6 and then optimized by model fitting.
- d) Values were optimized by model fitting, considering ¹⁴C-concentration profile in adipose tissues.

DMD #31914

Table 2 ¹⁴C-Levels in tissues of male rats during and after repeated oral administration of [dichlorophenyl-¹⁴C]pyridalyl at a rate of 5 mg/kg/day daily for 14 successive days.

Tissue	¹⁴ C concentration(μg pyridalyl equivalent/g tissue)													
	Days after the first administration													
	1day		6day		10day		14day		17day		20day		27day	
Adrenals	0.26	± 0.120	0.90	± 0.781	1.65	± 0.173	1.55	± 0.173	1.23	± 0.538	0.66	± 0.159	0.38	± 0.146
Blood	0.02	± 0.013	0.09	± 0.010	0.06	± 0.004	0.10	± 0.027	0.03	± 0.011	0.01	± 0.002	<0.01	
Plasma	0.03	± 0.019	0.15	± 0.008	0.09	± 0.010	0.13	± 0.019	0.04	± 0.018	0.02	± 0.003	<0.01	
Red blood cells	<0.01		0.04	± 0.011	0.03	± 0.005	0.03	± 0.006	<0.01		<0.01		<0.01	
Brain	0.03	± 0.007	0.07	± 0.003	0.09	± 0.012	0.11	± 0.006	0.02	± 0.002	0.02	± 0.004	0.01	± 0.011
Adipose tissue (Brown)	5.42	± 2.881	42.21	± 8.750	51.77	± 11.785	57.50	± 5.529	24.58	± 6.797	10.06	± 4.065	5.08	± 2.382
Adipose tissue (Perirenal)	1.87	± 1.473	23.35	± 3.185	42.06	± 9.938	43.11	± 3.840	37.87	± 5.731	30.17	± 3.017	19.45	± 3.870
Adipose tissue (Testicular)	1.73	± 1.402	19.30	± 2.303	31.58	± 1.367	40.12	± 6.263	34.44	± 6.673	29.39	± 4.817	21.56	± 0.873
Heart	0.05	± 0.028	0.26	± 0.045	0.31	± 0.093	0.43	± 0.159	0.11	± 0.012	0.15	± 0.079	0.04	± 0.016
Kidneys	0.25	± 0.100	1.33	± 0.270	1.07	± 0.023	1.34	± 0.396	0.43	± 0.147	0.47	± 0.044	0.21	± 0.184
Liver	1.12	± 0.614	4.32	± 0.893	4.35	± 0.602	5.60	± 1.263	1.35	± 0.107	0.77	± 0.106	0.25	± 0.043
Lungs	0.12	± 0.031	0.42	± 0.123	0.85	± 0.453	0.70	± 0.189	0.30	± 0.095	0.13	± 0.026	0.09	± 0.047
Muscle	0.04	± 0.025	0.16	± 0.047	0.23	± 0.077	0.26	± 0.059	0.14	± 0.030	0.10	± 0.033	0.07	± 0.035
Skin	0.38	± 0.199	2.61	± 1.817	5.95	± 2.364	4.23	± 1.666	3.12	± 1.870	3.09	± 0.731	1.59	± 0.979
Spleen	0.03	± 0.011	0.14	± 0.025	0.23	± 0.064	0.24	± 0.023	0.09	± 0.020	0.09	± 0.008	0.04	± 0.011
Testes	0.04	± 0.014	0.11	± 0.018	0.12	± 0.014	0.12	± 0.014	0.05	± 0.010	0.07	± 0.047	0.03	± 0.003
Thymus	0.09	± 0.023	0.37	± 0.134	1.38	± 0.235	1.42	± 0.323	0.20	± 0.084	0.99	± 0.577	0.18	± 0.076
Thyroids	0.60	± 0.309	2.02	± 1.314	3.32	± 1.050	3.76	± 1.880	0.79	± 0.475	0.95	± 0.124	0.32	± 0.288

Data are mean ± standard deviation values for three animals.

DMD #31914

Table 3 ^{14}C -Levels in tissues of female rats during and after repeated oral administration of [dichlorophenyl- ^{14}C]pyridalyl at a rate of 5 mg/kg/day daily for 14 successive days.

Tissue	^{14}C concentration(μg pyridalyl equivalent/g tissue)													
	Days after the first administration													
	1day	6day	10day	14day	17day	20day	27day	1day	6day	10day	14day	17day	20day	27day
Adrenals	0.33 ± 0.089	1.77 ± 0.468	1.89 ± 0.401	2.00 ± 0.191	1.05 ± 0.219	0.63 ± 0.236	0.41 ± 0.008							
Blood	0.03 ± 0.007	0.07 ± 0.041	0.12 ± 0.015	0.11 ± 0.054	0.02 ± 0.004	<0.01	<0.01							
Plasma	0.05 ± 0.007	0.10 ± 0.040	0.18 ± 0.034	0.16 ± 0.059	0.03 ± 0.008	0.01 ± 0.003	<0.01							
Red blood cells	<0.01	0.02 ± 0.013	0.04 ± 0.016	0.04 ± 0.018	<0.01 ±	<0.01	<0.01							
Brain	0.02 ± 0.018	0.05 ± 0.013	0.07 ± 0.004	0.07 ± 0.006	0.02 ± 0.006	<0.01	<0.01							
Adipose tissue (Brown)	7.00 ± 4.467	38.88 ± 4.137	31.94 ± 5.094	33.70 ± 10.748	20.07 ± 5.286	6.87 ± 2.657	4.80 ± 1.053							
Adipose tissue (Perirenal)	1.96 ± 1.011	16.92 ± 2.312	26.69 ± 4.428	32.36 ± 4.996	38.37 ± 10.856	25.88 ± 5.259	19.89 ± 1.283							
Heart	0.07 ± 0.013	0.23 ± 0.046	0.25 ± 0.042	0.30 ± 0.034	0.11 ± 0.034	0.08 ± 0.046	0.04 ± 0.017							
Kidneys	0.19 ± 0.033	0.56 ± 0.173	0.80 ± 0.140	0.90 ± 0.186	0.31 ± 0.038	0.27 ± 0.026	0.14 ± 0.018							
Liver	1.02 ± 0.377	2.71 ± 0.782	3.91 ± 0.528	3.74 ± 0.502	0.91 ± 0.146	0.51 ± 0.030	0.24 ± 0.030							
Lungs	0.09 ± 0.016	0.39	0.38 ± 0.083	0.74 ± 0.575	0.41 ± 0.333	0.11 ± 0.019	0.05 ± 0.004							
Muscle	0.04 ± 0.020	0.17 ± 0.035	0.17 ± 0.025	0.26 ± 0.039	0.13 ± 0.052	0.10 ± 0.048	0.05 ± 0.014							
Ovaries	0.51 ± 0.246	1.13 ± 0.301	1.48 ± 0.103	1.42 ± 0.202	0.84 ± 0.270	0.56 ± 0.111	0.62 ± 0.329							
Skin	0.31 ± 0.041	1.95 ± 0.281	2.48 ± 0.579	2.68 ± 0.960	3.48 ± 0.979	3.24 ± 1.157	1.07 ± 0.299							
Spleen	0.04 ± 0.008	0.13 ± 0.016	0.15 ± 0.019	0.18 ± 0.048	0.09 ± 0.029	0.06 ± 0.007	0.04 ± 0.009							
Thymus	0.08 ± 0.062	0.30 ± 0.149	0.25 ± 0.076	0.39 ± 0.173	0.34 ± 0.146	0.21 ± 0.182	0.06 ± 0.030							
Thyroids	0.40 ± 0.266	1.13 ± 0.263	1.92 ± 1.271	1.83 ± 0.666	1.28 ± 0.941	0.71 ± 0.416	0.26 ± 0.274							
Uterus	0.03 ± 0.002	0.12 ± 0.021	0.14 ± 0.037	0.13 ± 0.029	0.05 ± 0.008	0.08 ± 0.067	0.05 ± 0.023							

Data are the mean ± standard deviation values for three animals, except in the lung case at 6hr where the mean values are for two rats.

DMD #31914

Table 4 Biological half-lives of ^{14}C in tissues of male and female rats after repeated oral administration of [dichlorophenyl- ^{14}C]pyridalyl at a rate of 5 mg/kg/day daily for 14 successive days.

Tissue	Biological half-life time (day)							
	Male				female			
	α phase (calculation days)		β phase (calculation days)		α phase (calculation days)		β phase (calculation days)	
Adrenals	5	(Day 14-20)	9	(Day 20-27)	3	(Day 14-17)	7	(Day 17-27)
Blood	2	(Day 14-20)	-		1	(Day 14-17)	-	
Plasma	2	(Day 14-20)	-		2	(Day 14-20)	-	
Red blood cells	-		-		-		-	
Brain	1	(Day 14-17)	9	(Day 17-27)	2	(Day 14-17)	-	
Fat (Brown)	2	(Day 14-20)	7	(Day 20-27)	3	(Day 14-20)	14	(Day 20-27)
Fat (Perirenal)	-		10	(Day 17-27)	-		11	(Day 17-27)
Fat (Testicular)	-		15	(Day 17-27)	-		-	
Heart	2	(Day 14-17)	7	(Day 17-27)	2	(Day 14-17)	7	(Day 17-27)
Kidneys	2	(Day 14-17)	10	(Day 17-27)	2	(Day 14-17)	9	(Day 17-27)
Liver	1	(Day 14-17)	4	(Day 17-27)	1	(Day 14-17)	5	(Day 17-27)
Lungs	2	(Day 14-20)	13	(Day 20-27)	2	(Day 14-20)	6	(Day 20-27)
Muscle	4	(Day 14-17)	9	(Day 17-27)	3	(Day 14-17)	7	(Day 17-27)
Ovaries	-		-		4	(Day 14-17)	24	(Day 17-27)
Skin	-		9	(Day 14-27)	-		6	(Day 17-27)
Spleen	2	(Day 14-17)	10	(Day 17-27)	3	(Day 14-17)	8	(Day 17-27)
Testes	2	(Day 14-17)	14	(Day 17-27)	-		-	
Thymus	4	(Day 14-27)	-		5	(Day 14-27)	-	
Thyroids	1	(Day 14-17)	8	(Day 17-27)	4	(Day 14-20)	5	(Day 20-27)
Uterus	-		-		-		10	(Day 14-27)

-: Not calculated.

DMD #31914

Table 5 Comparison of metabolite distribution between 0-3 day and 11-14 day excreta of rats during repeated oral administration of [dichlorophenyl-¹⁴C]pyridalyl at a rate of 5 mg/kg/day daily for 14 successive days

	% of the total dose (% of total metabolites)			
	Male		Female	
	0-3day	11-14day	0-3day	11-14day
Feces				
pyridalyl	6.97	4.84	7.85	5.88
S-1812-DP	6.05 (62.1)	9.85 (59.4)	6.68 (63.6)	9.50 (63.2)
S-1812-Py-				
OH	0.14 (1.5)	0.07 (0.5)	0.15 (1.5)	0.29 (2.0)
HPHM	0.29 (3.0)	0.57 (3.5)	0.36 (3.4)	0.46 (3.1)
S-1812-AA	0.27 (2.8)	0.66 (4.0)	0.31 (3.0)	0.53 (3.5)
others	1.18 (12.1)	2.25 (13.6)	1.40 (13.3)	2.06 (13.7)
unextractable	1.28 (13.2)	2.18 (13.2)	1.30 (12.4)	1.76 (11.7)
subtotal	16.18	20.44	18.05	20.49
Urine				
polar	0.49 (5.0)	0.89 (5.4)	0.25 (2.4)	0.34 (2.3)
others	0.04 (0.4)	0.09 (0.6)	0.05 (0.5)	0.10 (0.6)
subtotal	0.53	0.99	0.30	0.44
Total	16.71	21.42	18.36	20.93

Downloaded from dmd.aspetjournals.org at ASPET Journals on April 21, 2021

DMD #31914

Table 6 Amounts of metabolites in whole blood, perirenal adipose tissue, kidneys, liver, and lungs of rats after repeated oral administration of [dichlorophenyl-¹⁴C]pyridalyl at a rate of 5mg/kg/day daily for 14 successive days

	Amounts of metabolite (µg equivalent of pyridalyl/g wet tissues)									
	Whole blood		Adipose tissue (Perirenal)		Kidneys		Liver		Lungs	
	Male	Female	Male	Female	Male	Female	Male	Female	Male	Female
pyridalyl	0.03	0.03	38.96	31.11	0.24	0.15	1.67	0.23	0.43	0.46
S-1812-DP	0.01	0.01	1.87	0.46	0.14	0.03	0.23	0.14	0.03	<0.01
S-1812-Py- OH	0.00	<0.00	0.59	0.41	<0.05	<0.02	0.06	<0.06	<0.01	<0.01
HPHM	0.00	0.01	<0.36	0.39	<0.04	0.04	0.08	<0.05	0.06	0.02
S-1812-AA	0.05	0.05	0.73	<0.36	0.45	0.29	2.12	1.30	0.03	0.04
others	0.01	0.02	0.97	0.00	0.35	0.14	0.69	1.53	0.04	0.14
unextractable	0.00	0.00	0.00	0.00	0.15	0.24	0.74	0.54	0.10	0.08
Total	0.10	0.11	43.11	32.36	1.34	0.90	5.60	3.74	0.70	0.74

Figure 1

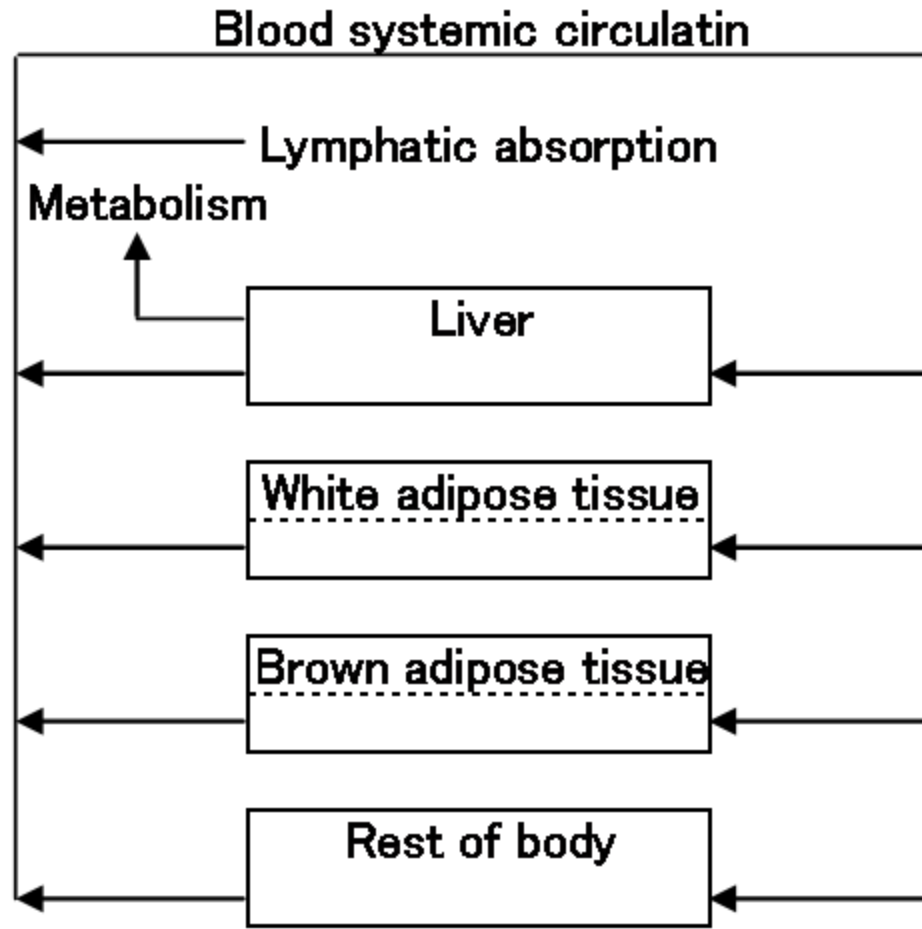


Figure 2

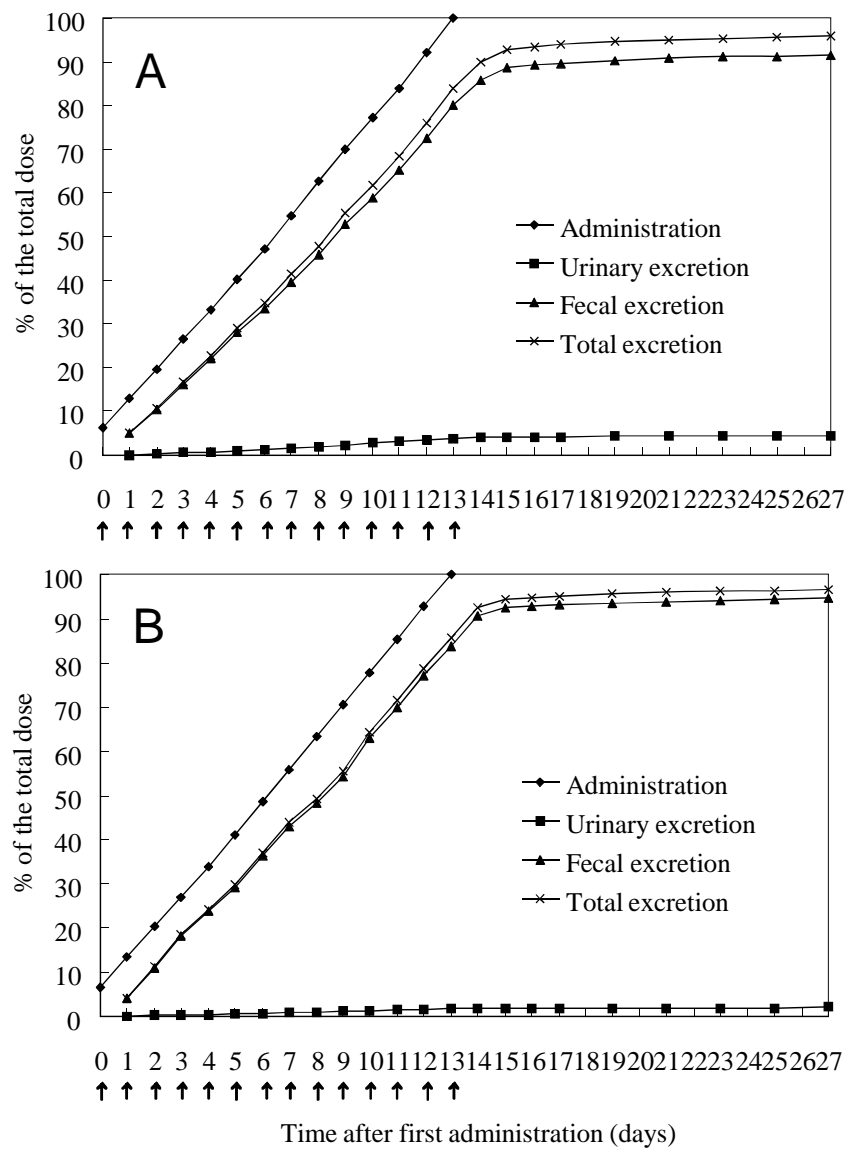


Figure 3

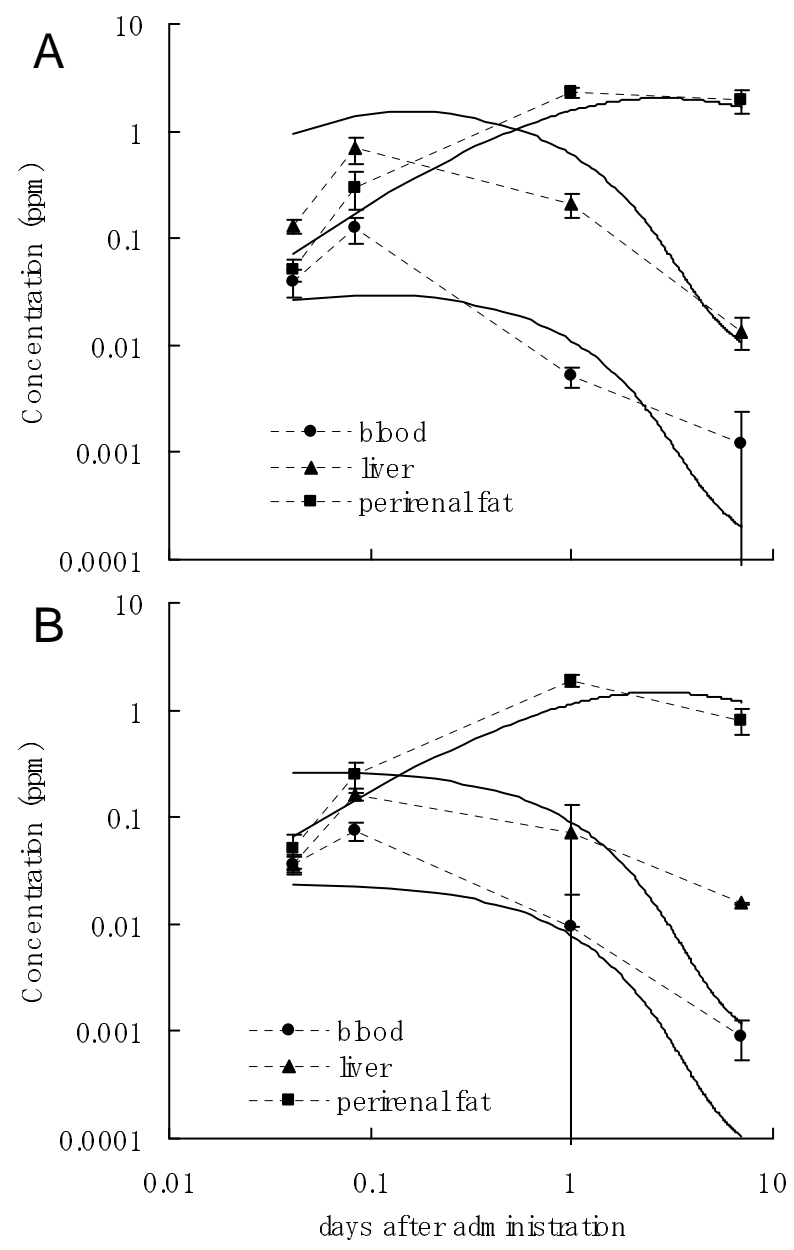


Figure 4

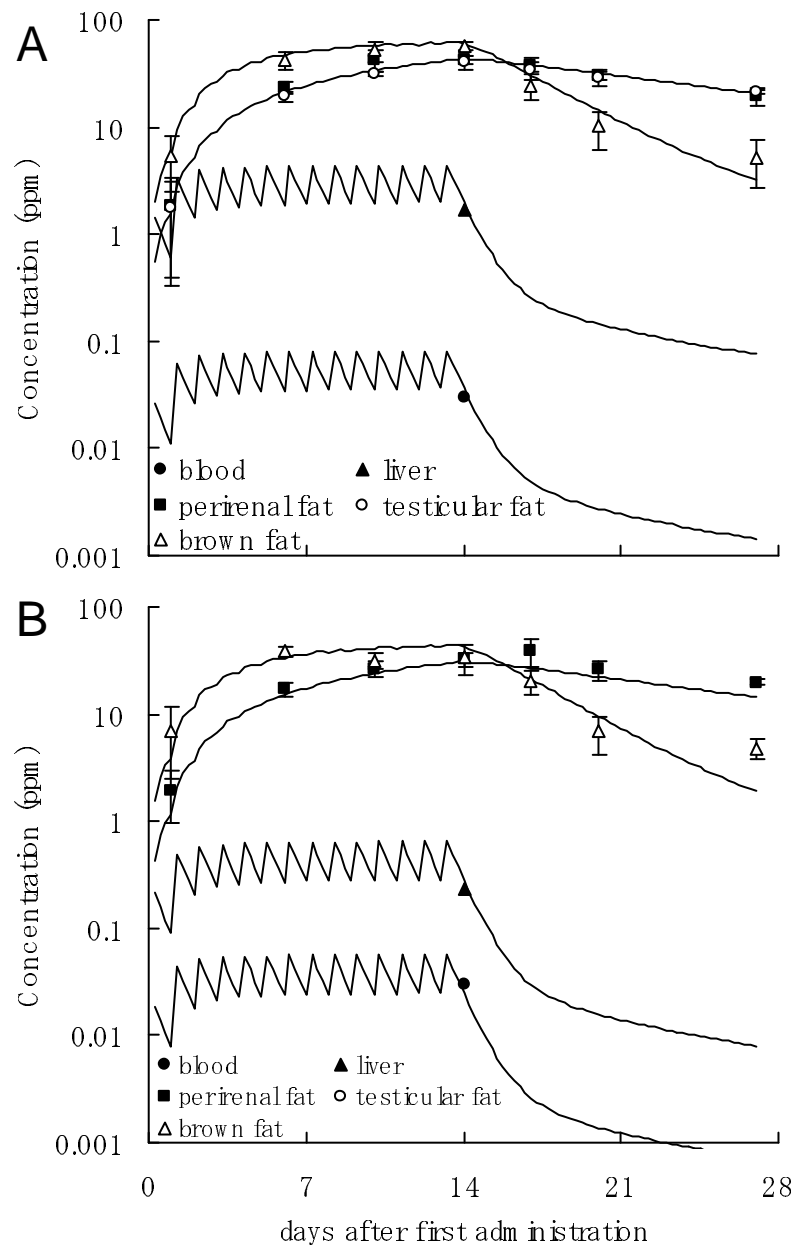


Figure 5

